

RESEARCH

Open Access



Electroacupuncture negatively regulates the Nesfatin-1/ERK/CREB pathway to alleviate HPA axis hyperactivity and anxiety-like behaviors caused by surgical trauma

Jiayuan Zheng¹ , Yu Wang¹ , Chi Zhang² , Anjing Zhang^{3,4}, Yuxiang Zhou¹, Yunhua Xu¹, Jin Yu¹ and Zhanzhuang Tian^{1*}

Abstract

Background Hyperactivity of the hypothalamic–pituitary–adrenal (HPA) axis constitutes a pivotal response by surgical trauma, manifesting as a critical aspect of the acute stress reaction. This hyperactivity resulted in adverse surgical outcomes and is often associated with increased postoperative anxiety. Increased evidence suggests that Nesfatin-1 plays a crucial role in stress responses and stress-related psychiatric disorders. Electroacupuncture (EA) is widely used to alleviate stress responses and anxiety, although its mechanism of action remains unclear. This study aimed to assess the mechanisms by which hypothalamic Nesfatin-1 contribute to the alleviation of HPA axis hyperactivity and anxiety by EA.

Methods Partial hepatectomy (HT) was performed to simulate surgical trauma, and EA was applied at Zusanli (ST36) and Sanyinjiao (SP6). The levels of hypothalamic Nesfatin-1, c-Fos, and corticotropin-releasing hormone (CRH) were detected, and serum adrenocorticotrophic hormone (ACTH) and corticosterone (CORT) were regarded as indicators of HPA axis activity. Anxiety levels were assessed through open field tests (OFT), elevated plus maze (EPM), and light–dark box tests (LDBT). To investigate the role of Nesfatin-1, its expression was modulated using stereotactic viral injections or plasmid transfections. Transcriptome sequencing was employed to explore the downstream signaling pathways of Nesfatin-1. Additionally, brain cannula implantation was performed to facilitate targeted drug administration.

Results Our findings demonstrated that EA reduced the hypothalamic overexpression of CRH and Nesfatin-1, as well as serum levels of ACTH and CORT. Additionally, it alleviated anxiety-like behaviors resulting from surgical trauma. We observed that overexpression of Nesfatin-1 in the hypothalamic paraventricular nucleus (PVN) triggered hyperactivity of the HPA axis and anxiety. Conversely, knocking down Nesfatin-1 in the PVN reversed these effects caused by surgical trauma. Transcriptome sequencing identified the extracellular regulated protein kinases (ERK)/cAMP-response element binding protein (CREB) pathway as a key mediator in the impacts of surgical trauma and EA on the hypothalamus. Both in vivo and in vitro studies showed that overexpression of Nesfatin-1 activated the ERK/CREB pathway. Furthermore, administering ERK or CREB inhibitors into the PVN mitigated HPA axis hyperactivity and anxiety-like behaviors induced by surgical trauma. Finally, EA was observed to decrease the phosphorylation levels of ERK and CREB in the PVN.

*Correspondence:

Zhanzhuang Tian

tianzv@shmu.edu.cn

Full list of author information is available at the end of the article



© The Author(s) 2024, corrected publication 2024. **Open Access** This article is licensed under a Creative Commons Attribution 4.0 International License, which permits use, sharing, adaptation, distribution and reproduction in any medium or format, as long as you give appropriate credit to the original author(s) and the source, provide a link to the Creative Commons licence, and indicate if changes were made. The images or other third party material in this article are included in the article's Creative Commons licence, unless indicated otherwise in a credit line to the material. If material is not included in the article's Creative Commons licence and your intended use is not permitted by statutory regulation or exceeds the permitted use, you will need to obtain permission directly from the copyright holder. To view a copy of this licence, visit <http://creativecommons.org/licenses/by/4.0/>. The Creative Commons Public Domain Dedication waiver (<http://creativecommons.org/publicdomain/zero/1.0/>) applies to the data made available in this article, unless otherwise stated in a credit line to the data.

Conclusion EA alleviates HPA axis hyperactivity and anxiety-like behaviors caused by surgical trauma through inhibition of Nesfatin-1/ERK/CREB pathway in the hypothalamus.

Keywords HPA axis, Anxiety, Nesfatin-1/ERK/CREB pathway, Surgical trauma, Electroacupuncture

Introduction

Surgical procedures hold a crucial role in modern medicine, encompassing a wide array of applications such as the resection of cancerous tissues, repair of traumatic injuries, and treatment of heart diseases [1]. However, during the surgical process, patients are exposed to trauma, anesthesia, and pain, leading to the hyperactivity of the hypothalamic–pituitary–adrenal (HPA) axis. This represents a significant manifestation of the stress response triggered by surgical trauma [2]. Typically, the hyperactivity of the HPA axis is characterized by an increased synthesis and release of corticotropin-releasing hormone (CRH) in the hypothalamic paraventricular nucleus (PVN), along with elevated serum levels of adrenocorticotrophic hormone (ACTH) and corticosterone (CORT) [3]. While the activation of the HPA axis is necessary for maintaining homeostasis, excessive hyperactivity of the HPA axis can result in severe and potentially life-threatening consequences [4]. These adverse effects include high metabolism, organ damage [5], systemic inflammatory responses, immune suppression [6], and psychological symptoms such as anxiety and delirium [1, 7]. Research indicates that patients experiencing postoperative anxiety often have prolonged hospital stays, lower postoperative satisfaction, poorer compliance with rehabilitation and treatment, and slower recovery rates [8]. Given the current lack of specific methods for the prevention and treatment of excessive stress responses following surgery and major trauma, exploring the mechanisms underlying their development and maintenance, as well as seeking solutions, holds significant clinical significance.

Acupuncture is one of the traditional Chinese therapeutic methods [9], and electroacupuncture (EA) represents a modern advancement of this practice. EA combines acupuncture stimulation with the subsequent electrophysiological effects, delivering pulsed stimulation with different waveforms to specific acupoints [10]. A substantial body of research suggests that acupuncture can improve perioperative complications, including intraoperative hemodynamic instability, immunosuppression [11], pain, nausea, vomiting, cognitive dysfunction, and anxiety [12–14]. Zusanli (ST36) and Sanyinjiao (SP6) are the most used acupoints for EA to alleviate hyperactivity of the HPA axis induced by acute stress [15]. Our previous studies also demonstrated that EA at these two acupoints can improve HPA axis hyperactivity

in partial hepatectomy (HT) mice [16]. Although previous studies have indicated a significant alleviating effect of EA on the HPA axis hyperactivity and anxiety induced by surgical trauma [17–19], the molecular mechanisms underlying the therapeutic effects of EA still remain largely unknown.

Nesfatin-1 was initially discovered as a neuropeptide with anorexigenic effects, and as research progressed, its role in mediating stress and stress-related anxiety has been increasingly reported [20]. Nesfatin-1 is derived from nucleobindin2 (NUCB2) through cleavage [21], and it is massively distributed in the PVN [22]. It effects through binding to G protein-coupled receptors that have not yet been identified [23]. Studies have shown that administration of Nesfatin-1 into the lateral ventricle or intravenously in rats elevates serum ACTH and CORT levels [24, 25], which is associated with heightened anxiety [26]. Conversely, administration of Nesfatin-1 antibody or blockade of endogenous Nesfatin-1 centrally can attenuate its anxiety-like behaviors [27]. These findings indicate that central Nesfatin-1 is crucial for the activation of the HPA axis and the development of anxiety under stress.

In the present study, we observed that EA alleviates the hyperactivity of the HPA axis and anxiety resulting from surgical trauma by inhibiting the overexpression of Nesfatin-1 in the hypothalamus. Employing transcriptomic sequencing techniques, we further identified that the excessive secretion of CRH, induced by surgical trauma, is mediated by the Nesfatin-1/extracellular regulated protein kinases (ERK)/cAMP-response element binding protein (CREB) pathway. Furthermore, EA demonstrates inhibitory effects on this pathway. This article innovatively investigates how EA ameliorates anxiety triggered by traumatic stress through the regulation of central Nesfatin-1 and its mediated function in the HPA axis. It offers a promising therapeutic strategy and identifies potential targets for treating endocrine and mental disorders associated with clinical surgery.

Materials and methods

Experimental animals

C57BL/6 J mice (male, 7–8 weeks, 20–23 g), were purchased from Yuxiu Biotechnology Co., Ltd. (Shanghai, China). All of them were housed in a room with a temperature of 22–24 °C, humidity ranging from 50 to 60%, and a 12-h light/dark cycle, with free access to food and

water. After one week of acclimatization to the environment, experiments were conducted. All animal experiments were reviewed and approved by the Ethics Committee for Laboratory Animals, School of Basic Medical Sciences, Fudan University (20240229–050).

Partial hepatectomy model

The mice were divided into Intact, partial hepatectomy (HT), and HT+EA groups. All animals underwent 30 min of daily restraint adaptation for a period of 3 days. The surgical trauma model used in this experiment is as described earlier [17]. In brief, after intraperitoneal injection of 0.2 mL/10 g Avertin for anesthesia, a surgical incision was made in mice, approximately 3 cm long along the midline from the xiphoid process to the pubic symphysis. The abdominal cavity was fully opened, and 10% of the liver was resected from the left lobe. After removing 10% of the liver lobe, hemostasis was immediately achieved using a disinfected dry cotton ball for approximately 5 min. Finally, the abdominal cavity was sutured. Throughout the surgical procedure, environmental temperature and aseptic techniques were strictly controlled, and the surgery was conducted from 8:00 to 10:00 in the morning.

EA

Mice in each group were habituated to the self-made fixing devices (50 mL centrifuge tubes with enough holes to make sure mice could breathe normally and facilitate EA stimulation) once a day for three consecutive days before the first EA. In the EA procedure, mice were safely restrained and kept awake, while the Intact and HT groups were also restrained but received no other interventions. The acupoints chosen for EA were “Zusanli” (ST36, located on the outer side below the knee joint, about 2 mm below the head of the fibula [28]) and “Sanyinjiao” (SP6, located 5 mm below the head of the fibula and 2 mm outside the anterior tibial tubercle) on the right hind limb. The EA occurred on the morning of the day before surgery and immediately after the abdominal closure [29]. The 0.5-inch (0.22×13 mm) acupuncture needles (Hua Tuo, Suzhou, China) were used, inserted vertically into the ST36 to a depth of approximately 5 mm, and inserted horizontally from bottom to top into the ST6 to a depth of about 5 mm. Both acupoints were connected to a HANS Acupoint Nerve Stimulator (LH202H, Beijing, China). The EA parameters were set as follows: dense-sparse wave, frequency of 2–15 Hz, intensity ranging from 1–2 mA, with slight tremors observed in the lower limbs as the endpoint, and a duration of 30 min. At the end of the experiment (24 h post-HT), animals in all groups were decapitated following

administration of Avertin. Blood was then collected via retro-orbital bleeding, and the hypothalamus was harvested on ice.

Enzyme linked immunosorbent assay

After peripheral blood collection via retro-orbital bleeding, centrifugation was conducted at 4 °C and 3000 rpm for 30 min. The upper serum layer was collected post-centrifugation. Enzyme-linked immunosorbent assay (ELISA) kits, purchased from Shanghai Lengton Biotechnology Co., Ltd. (Shanghai, China), were employed for the quantification of plasma ACTH and CORT levels.

Real-time polymerase chain reaction

Total RNA was isolated from hypothalamic tissues using TRIzol Reagent (15596026, Life Technologies, USA). Subsequently, the RNA was reverse transcribed into cDNA using the PrimeScript RT Reagent Kit (RR036A, Takara, Japan) according to the manufacturer's instructions. PCR was performed with the SYBR Premix Ex Taq kit (RR420B, Takara, Japan) and the QuantStudio 3 Real-Time PCR System (ThermoFisher, USA). The reaction volume consisted of 10 µL SYBR Premix Ex Taq mixture, 0.8 µL primer mixture, 2 µL cDNA template, and 6.8 µL ddH₂O. Transcript levels were normalized to the GAPDH within the same sample. The mRNA primers were synthesized by Shanghai Sangon Biotech Co., Ltd. (Shanghai, China).

The primer sequences were as follows: NUCB2 (Forward: 5' AAG AAG TAG GAA GAC TGC GGA TGC3'; Reverse: 5' AGG ATT CTG GTG GTT CAG GTG TTC3'); CRH (Forward: 5' CTG TCG TCC TGC CTG CCT TG3'; Reverse: 5' TTC ACC CAT GCG GAT CAG AAC C3'); GAPDH (Forward: 5' AGA AGG TGG TGA AGC AGG CAT C3'; Reverse: 5' CGA AGG TGG AAG AGT GGG AGT TG3'). The relative mRNA levels were analyzed using the 2^{-ΔΔCt} method, normalized to GAPDH.

Western blot

At 24 h post-surgery, hypothalamic tissues of mice were collected after the administration of Avertin. The hypothalamic tissues were lysed using RIPA lysis buffer (Biosharp, China) containing a mixture of proteinase and phosphatase inhibitors (Beyotime, China) and subjected to ultrasonic homogenization. The supernatant was centrifuged at 4 °C, 12,000 rpm for 20 min. Protein concentration was determined using a BCA assay kit (Beyotime, China). Equal amounts of protein were separated by 12% SDS-PAGE (ACE, China) and transferred onto PVDF membranes (Millipore, German). The membranes were blocked with TBST containing 5% skimmed milk powder or Rapid Protein-Free Blocking Buffer (ACE, China).

Subsequently, the membranes were incubated overnight at 4 °C with primary antibodies against CRH (10944-1-AP, anti-rabbit, 1:1000, Proteintech), Nesfatin-1 (AF6895, anti-sheep, 1:1000, R&D), β -tubulin (10094-1-AP, anti-rabbit, 1:10000, Proteintech), phosphor-ERK1/2 (4370, anti-rabbit, 1:1000; Cell Signaling Technology), ERK1/2 (4695, anti-rabbit, 1:2000; Cell Signaling Technology), phosphor-CREB Ser133 (9198S, anti-rabbit, 1:1000; Cell Signaling Technology), and CREB (12208-1-AP, anti-rabbit, 1:1000; Proteintech). Following washes with TBST, the membranes were incubated with secondary antibodies, either HRP-conjugated goat anti-rabbit (L-3012, 1:10000; SAB) or rabbit anti-sheep (AS023, 1:10000; ABclonal). Signal visualization was performed using ECL (Epizyme, China), and protein bands were detected using the Amersham ImageQuant 800 Protein Blot Imaging System. ImageJ software was employed for quantifying the grayscale values of the bands, and the relative expression of the target proteins was calculated based on the grayscale values of internal reference bands.

Open field tests

The anxiety levels of mice were assessed using the open field tests (OFT) 24 h after the surgery [30]. The apparatus consisted of a square arena with opaque plastic walls (length=width=50 cm, height=40 cm). Each mouse was gently placed in the center of the arena, and allowed to explore the area for 10 min, during which their movement trajectory was recorded. Parameters evaluated included time spent in the central zone, central zone cross counts, the ratio of central distance to total distance, and grooming episode. After each trial, residual odors were eliminated using 75% ethanol.

Elevated plus maze

Elevated plus maze (EPM) apparatus consists of two enclosed arms (length 20 cm, width 4 cm, height 12 cm) and two similar open arms arranged in a cross. A 10-min test is employed to determine the time spent in the open arms and entries made into the open arms. The apparatus is cleaned with 75% ethanol to eliminate residual odors left by the preceding animal.

Light-dark box tests

The apparatus used for this experiment consisted of a box (35×25×30 cm) divided into two compartments: one-third of the box (dark) and two-thirds of the box (light). Mice were placed in the light compartment and allowed to freely explore the room for 10 min. A video camera was utilized to record the mouse's movements in the light area. Anxiety-like behaviors in mice were assessed based on the time spent and the distance traveled in the

light area. The apparatus was cleaned with 75% ethanol to eliminate residual odors left by the preceding animal.

Immunofluorescence

Mouse coronal brain slices (thickness 40 μ m) were obtained, and selected slices were subjected to immunofluorescent staining. In brief, brain samples were incubated or co-incubated with antibodies against c-Fos (226008, anti-rabbit, 1:400, SYSY), Nesfatin-1 (AF6895, anti-sheep, 1:200, R&D), CRH (C36806, anti-rabbit, 1:200, SAB), or phosphor-ERK1/2 (4370, anti-rabbit, 1:200, Cell Signaling) at 4 °C overnight. The slices were then incubated with the respective secondary antibodies, Alexa Fluor 488 (A-21206, 1:1000, ThermoFisher) or Alexa Fluor 594 (A-11016, 1:1000, ThermoFisher), at room temperature in the dark for 2 h. Visualization was conducted using the integrated fluorescence microscopy system BZ-X (KEYENCE, Japan). For quantitative analysis of immunostained cells, ImageJ software was used to count the numbers of CRH, Nesfatin-1, c-Fos, phosphor-ERK1/2 positive cells, and co-labeled cells within a 400 μ m² area adjacent to the third ventricle (3 V).

Virus injection

After intraperitoneal injection of Avertin for anesthesia, mice were placed in a stereotaxic apparatus. Following fixation, the hair on the head was shaved, and the surgical site was treated with a dilute iodine solution. An incision was made in the scalp, and the surgical area was swabbed with a surgical sponge soaked in hydrogen peroxide until the skull was exposed. The location of the PVN of the hypothalamus was (AP 0.6 mm, ML \pm 0.2 mm) [29, 31]. Using a dental drill, a hole was slowly drilled into the skull, and a Hamilton 2.5 μ L microsyringe, coupled with a glass electrode, was used to extract the virus. The viruses used were rAAV2/9-CMV-Nesfatin-1-EGFP-WPRE-hGH or rAAV2/9-U6-CMV-shRNA (scramble)-mCherry-SV40 obtained from BrainVT A Co., Ltd. (Wuhan, China). The virus was slowly inserted into the PVN to a depth of 4.5 mm at a rate of 40 nL/min, and a total injection volume of 200 nL. After the injection was completed, a 5-min waiting period was observed to prevent viral overflow. Subsequently, the skin on the head was sutured.

Cell culture and plasmid transfection

The mouse neuroblastoma-2a (N2a) cells were obtained from the Center for Excellence in Molecular Cell Science, Chinese Academy of Sciences, and cultured in DMEM (Biosharp, China) supplemented with 10% fetal bovine serum, 50 units/mL penicillin, and 100 μ g/mL streptomycin (Biosharp, China) at 37 °C in a humidified atmosphere with 5% CO₂.

Overexpression or knockdown of Nesfatin-1 in N2a cells was achieved through plasmid transfection. The plasmid backbone is consistent with the viral nucleic acid framework. For transfection, N2a cells were plated at 60% density in 6-well culture plates, and JetPrime transfection reagent (PolyPlus Transfection, France) was used. mRNA or protein was extracted 48 h post-transfection, with a transfection efficiency of approximately 75%. In interventions with inhibitors, SCH772984 (HY-50846, MCE) or 666-15 (HY-101120, MCE) was added 24 h after plasmid transfection, following the same steps as before.

Transcriptome sequencing

Sprague–Dawley (SD) rats (male, 7–8 weeks, 180–220 g) were purchased from the Slack Laboratory Animal Center (Shanghai Branch of the Chinese Academy of Sciences, Shanghai, China). Rats were in good health without any pre-existing conditions that could affect the study results. They successfully adapted to the experimental environment for one week before the experiment. Rats were randomly assigned to the three groups (Intact, HT, EA) using a random number generator. To ensure objectivity and reduce bias, all experimental assessments and subsequent analyses were conducted by researchers blinded to the group allocations. The groups were coded, and the code was not revealed until the completion of the data analysis. The samples were prepared using the Seq-RNA sequencing method provided by Novo Gene Biotech Co. Ltd. (Beijing, China). Three SD rats from each group were included. The surgical and EA procedures were identical to those performed in mice. 24 h after HT, the hypothalamic tissues were isolated from the rats, preserved in RNA storage solution, and sent to Novo Gene Biotech Company for subsequent analysis. The construction of cDNA libraries, library purification, and transcriptome sequencing were conducted following the protocols provided by Novo Gene Biotech Company. The normalized RNA count data was used for subsequent Principal Component Analysis (PCA) in R. Differential Expression analysis for RNA-Seq data was performed using R/Bioconductor package edgeR. The threshold of significance was set as a p value < 0.05 to find transcriptionally regulated genes. Heatmaps were made using R/Bioconductor package pheatmap (<https://CRAN.R-project.org/package=pheatmap>). Volcano plots were made using ggplot2 in R.

Stereotactic cannula implantation and PVN administration

The bilateral PVN cannulation in mice was performed under Avertin anesthesia. The drug delivery system was designed by RWD Life Science Co., Ltd. (RWD, Shenzhen, China). Modeling and drug administration were carried out two weeks after the cannulation. On the day

before surgery and immediately after surgery, mice were administered ERK1/2 inhibitor SCH772984 (0.1 nmol/ μ L, 0.5 μ L/side, HY-50846, MCE), CREB inhibitor 666-15 (0.1 nmol/ μ L, 0.5 μ L/side, HY-101120, MCE), or normal saline (NS) at a rate of 0.1 μ L/min into the PVN [29]. After injection, the mice were left undisturbed for 5 min to allow for drug diffusion. All mice were euthanized under anesthesia 24 h after the last administration. Peripheral blood and hypothalamic tissue were collected and frozen for further experiments.

Statistical analysis

All data were analyzed using GraphPad prism 9.0 software. Data were presented as mean \pm SEM, and comparisons between two groups were performed using unpaired two-tailed t -tests. Multiple group comparisons were conducted using one-way ANOVA or two-way ANOVA. A p -value < 0.05 was considered statistically significant.

Results

EA alleviates the HPA axis hyperactivity and anxiety-like behaviors caused by surgical trauma

The experimental design and workflow are depicted in Fig. 1A, F. We assessed serum concentrations of ACTH and CORT, as well as CRH expression in the hypothalamus 24 h post-surgery to evaluate HPA axis activity. Anxiety-like behaviors were evaluated by the OFT, EPM, and light–dark box tests (LDBT). Compared to the Intact mice, the HT mice exhibited a significant increase in plasma levels of ACTH and CORT, as well as an increase in CRH mRNA and protein expression in the hypothalamus, and a higher count of CRH-positive cells in the PVN post-surgery. Interestingly, the combination of preoperative and postoperative EA significantly mitigated surgical trauma-induced hyperactivity of the HPA axis, as evidenced by substantial reductions in the expression levels of various HPA axis components (Fig. 1B–E, Fig. 2G).

The OFT results demonstrated that EA significantly reversed the decreased time spent in the central zone, reduced traveled distance in the central zone (normalized to total distance), decreased crossing counts of the central zone, and increased grooming episodes observed in HT mice (Fig. 1G–K). The EPM results indicated that EA significantly reversed the decreased time spent in the open arms and reduced entries into the open arms observed in HT mice (Fig. 1L, M). The LDBT results showed that EA significantly reversed the decreased time spent and traveled distance in the light area observed in HT mice (Fig. 1N, O). These results indicate that EA could alleviate the hyperactivity of the HPA axis caused by surgical trauma and further improve anxiety-like behaviors.

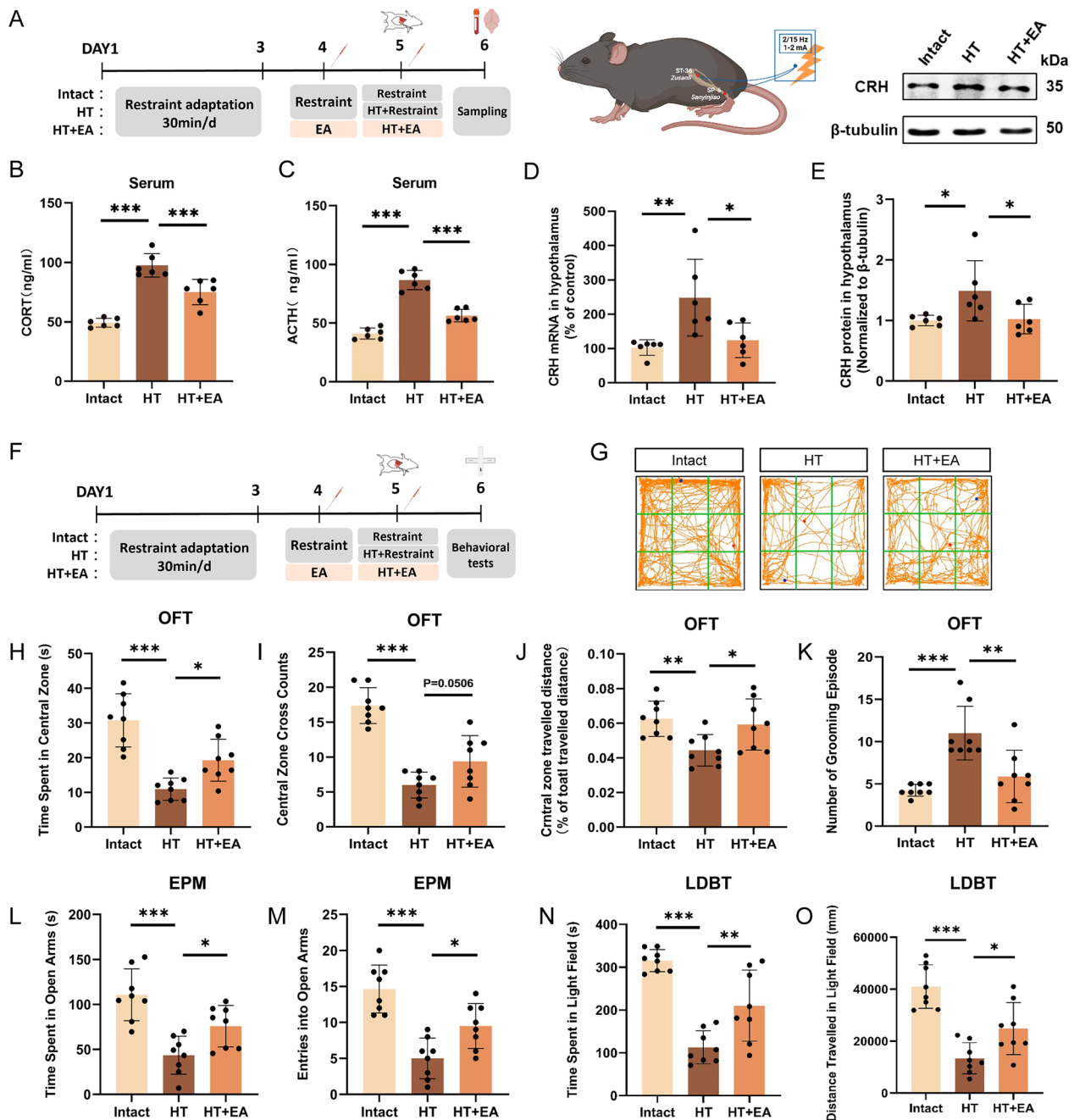


Fig. 1 EA alleviates surgery-induced HPA axis hyperactivity and anxiety. **A, F** Schematic representation of the HT model and EA protocol. **B, C** ELISA measurement of serum ACTH and CORT levels. **D, E** Quantification of CRH mRNA and protein in hypothalamus. Anxiety levels in mice post-surgery were assessed through the OFT (**G–K**), the EPM (**L, M**) and the LDBT (**N, O**). All data are shown as mean \pm SEM, $n = 6–8$ in each group, * $p < 0.05$, ** $p < 0.01$, *** $p < 0.001$

EA mitigates overexpression of hypothalamic Nesfatin-1 induced by surgical trauma

Given the crucial role of Nesfatin-1 in stress and stress-induced anxiety, our investigation concentrated on this peptide within the hypothalamus, exploring it as a potential target for EA intervention. Firstly, we performed

co-staining of Nesfatin-1 with c-Fos. At 24 h post-surgery, the HT mice showed elevated numbers of c-Fos-positive cells and their co-labeled with Nesfatin-1 in the PVN compared to the Intact mice. There was a significant reduction in the c-Fos expression and their co-labeled with Nesfatin-1 within PVN following EA. (Fig. 2A–C). In comparison to

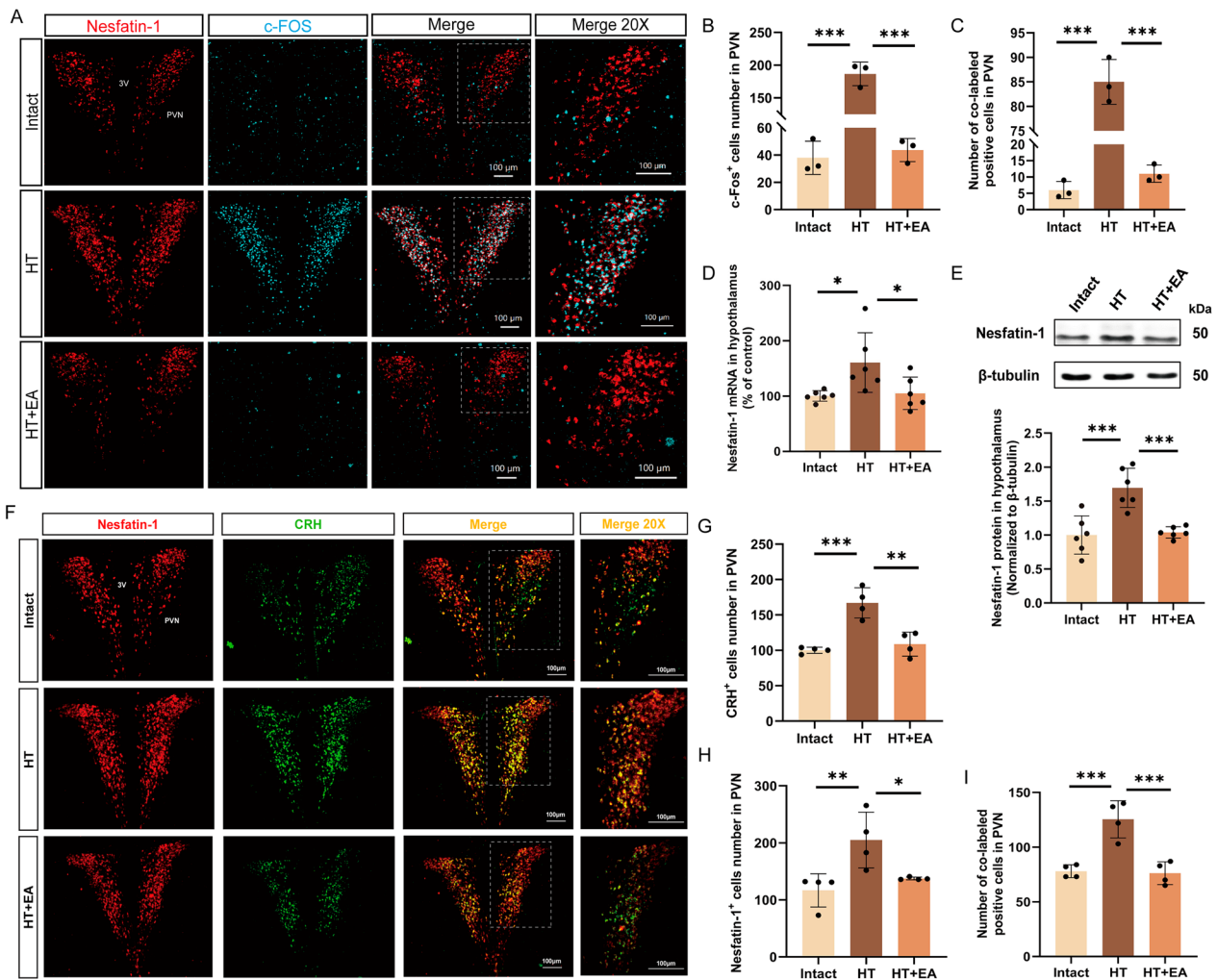


Fig. 2 EA alleviates surgical trauma-induced overexpression of Nesfatin-1 in the hypothalamus. **A** Immunofluorescence staining for Nesfatin-1 and c-Fos in the PVN at 24 h post-surgery in the Intact, HT, and EA+HT groups. Scale bar = 100 μ m. **B, C** Quantification of c-Fos-positive cells and their co-labeled with Nesfatin-1 in each group at 24 h post-surgery. **D, E** Expression levels of Nesfatin-1 mRNA and protein in the hypothalamus in each group. **F** Immunofluorescence staining for Nesfatin-1 and CRH in the PVN at 24 h post-surgery. Scale bar = 100 μ m. **G–I** Quantification of CRH-positive cells, Nesfatin-1-positive cells, and their co-labeled cells in each group. All data are shown as mean \pm SEM, $n = 3–6$ in each group, * $p < 0.05$, ** $p < 0.01$, *** $p < 0.001$

the Intact mice, the HT mice exhibited significant upregulation of Nesfatin-1 mRNA and protein levels in the hypothalamus, increased numbers of Nesfatin-1-positive cells, and their co-labeled with CRH in the PVN. These alterations were also effectively inhibited by EA (Fig. 2D–F, H, I). These data confirm that EA could directly regulate the overexpression of Nesfatin-1 induced by surgical trauma.

Knockdown of Nesfatin-1 expression in the PVN alleviates surgical trauma-induced HPA axis hyperactivity and anxiety-like behaviors

To further investigate the role of Nesfatin-1 in the adverse consequences of surgical trauma, we

administered AAV-shRNA targeting Nesfatin-1 into the PVN to achieve Nesfatin-1 knockdown (Fig. 3A). Three weeks post-virus injection, the area of virus infection was visualized (Fig. 3B), following which the mice were subjected to HT. In mice injected with AAV-mCherry (scramble), there were significant increases in the hypothalamic Nesfatin-1 mRNA and protein, CRH mRNA and protein, and serum levels of ACTH and CORT in the HT mice compared to the control mice (Fig. 3C–H). In mice injected with AAV-shRNA (Nesfatin-1), no significant differences were observed in these parameters when HT mice compared to the control mice (Fig. 3C–H).

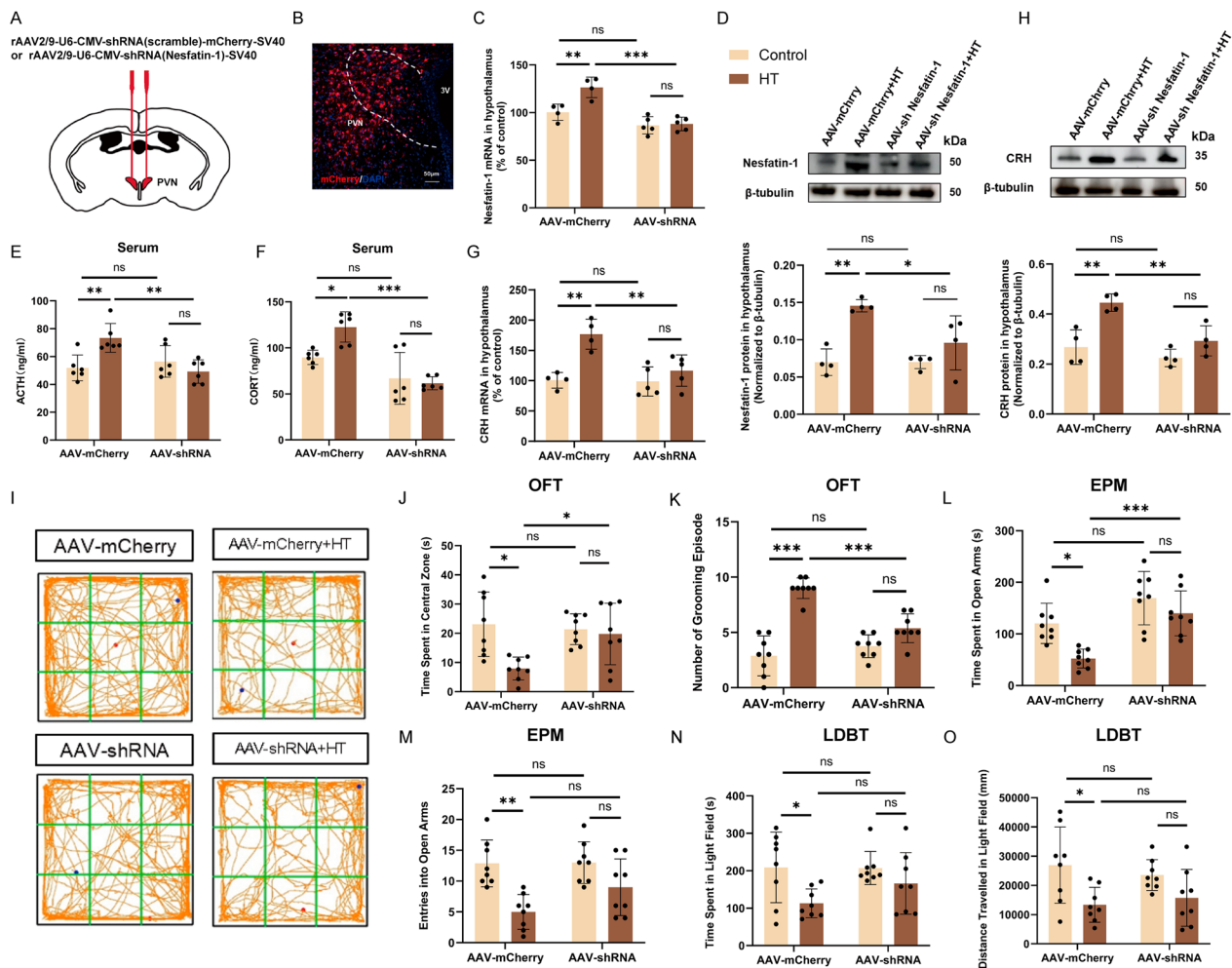


Fig. 3 Knockdown of Nesfatin-1 in PVN alleviates HPA axis hyperactivity and anxiety-like behaviors induced by surgical trauma. **A, B** Diagram illustrating the sites of virus injection. Scale bar = 50 μ m. **C, D** Expression levels of Nesfatin-1 mRNA and protein in the hypothalamus from different groups. **E, F** Serum levels of ACTH and CORT in different groups. **G, H** Expression levels of CRH mRNA and protein in the hypothalamus from different groups. OFT (**I–K**), EPM (**L, M**), and LDBT (**N, O**) were used to assess anxiety levels in different groups of mice. All data are shown as mean \pm SEM, $n = 4–8$ in each group, * $p < 0.05$, ** $p < 0.01$, *** $p < 0.001$

The OFT results showed that HT mice injected with scramble virus exhibited a significant decrease in time spent in central zone (Fig. 3I, J), while the grooming episodes significantly increased (Fig. 3K). The EPM results showed that HT mice injected with scramble virus exhibited a significant decrease in the time spent in the open arms and entries into the open arms (Fig. 3L, M). The LDBT results showed that HT mice injected with scramble virus exhibited a significant decrease in the time spent and distance traveled in the light area (Fig. 3N, O). However, when PVN Nesfatin-1 is knocked down, the aforementioned anxiety behaviors are alleviated (Fig. 3I–O). These results indicate that knockdown of Nesfatin-1 in the PVN could alleviate HPA axis hyperactivity and further anxiety-like behaviors caused by surgical trauma.

Overexpression of Nesfatin-1 in the PVN induces the HPA axis hyperactivity and anxiety-like behaviors

AAV-Nesfatin-1 was injected into the PVN to achieve overexpression of Nesfatin-1 (Fig. 4A). Three weeks post-virus injection, the infected area was observed (Fig. 4B). Compared to the AAV-GFP (scramble) group, mice in the AAV-Nesfatin-1 group showed a significant increase in Nesfatin-1 mRNA and protein levels in the hypothalamus (Fig. 4C, D), indicating successful overexpression of Nesfatin-1. Nesfatin-1 overexpression significantly elevated plasma ACTH and CORT levels, as well as hypothalamic CRH mRNA and protein levels (Fig. 4E–H). This suggests a positive regulatory effect of Nesfatin-1 on the HPA axis.

In the OFT, AAV-Nesfatin-1 mice showed a significant decrease in central zone cross counts compared to the AAV-GFP group (Fig. 4L), while total travelled

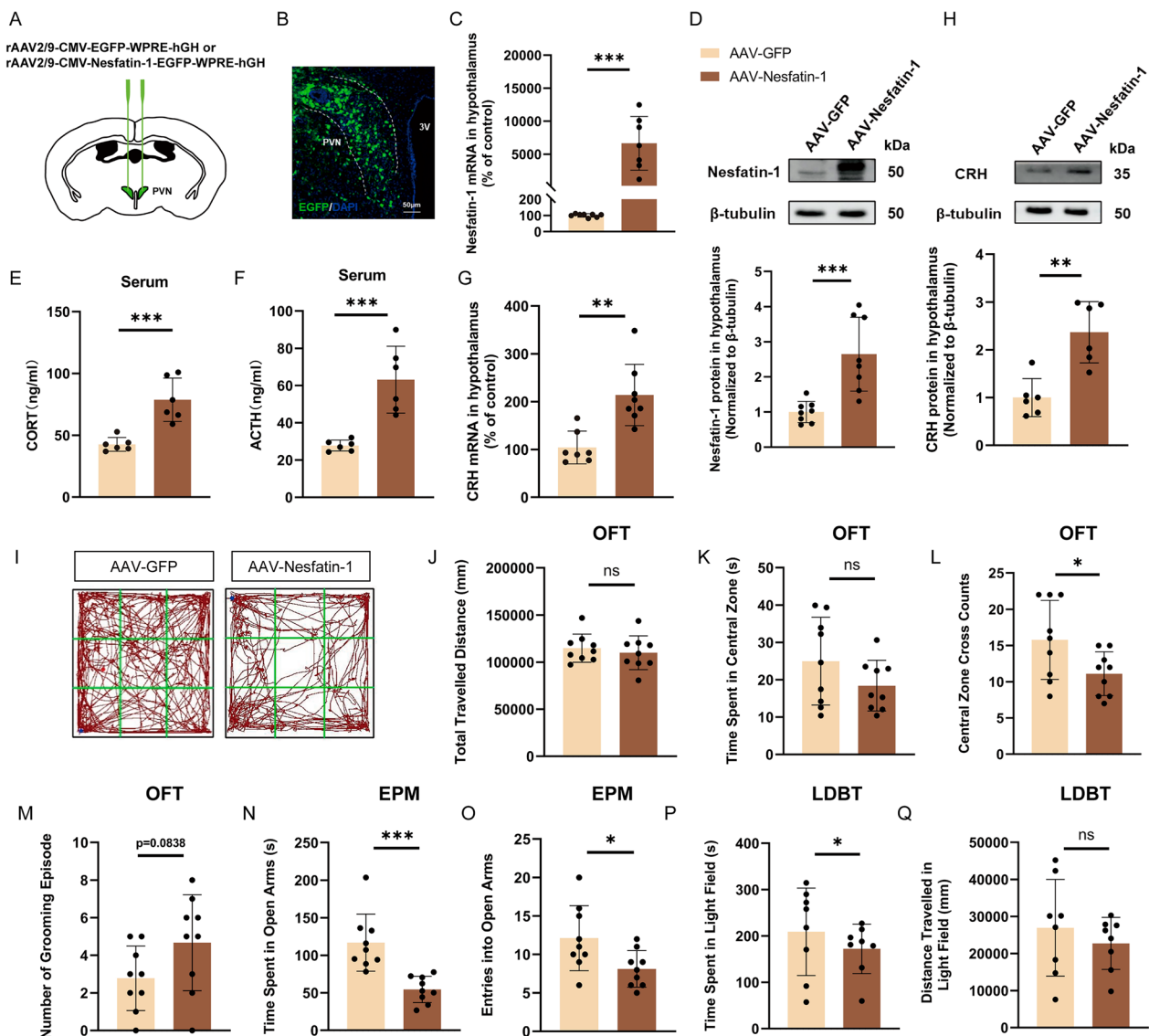


Fig. 4 PVN overexpression of Nesfatin-1 induces HPA axis hyperactivity and anxiety-like behaviors. **A, B** Diagram of virus injection sites. Scale bar = 50 μ m. **C, D** Expression levels of Nesfatin-1 mRNA and protein in the hypothalamus in each group. **E, F** Serum levels of ACTH and CORT in each group. **G, H** Expression levels of CRH mRNA and protein in the hypothalamus in each group. OFT (**I–M**), EPM (**N, O**), LDBT (**P, Q**, each group had one animal death) were used to assess anxiety levels in mice in each group. All data are shown as mean \pm SEM, $n=6-9$ in each group, * $p < 0.05$, ** $p < 0.01$, *** $p < 0.001$

distance, time spent in central zone and grooming episodes showed no significant difference (Fig. 4I–K, M). In the EPM, AAV-Nesfatin-1 mice exhibited a significant decrease in time spent on and entries into the open arms (Fig. 4N, O). LDBT results indicated that AAV-Nesfatin-1 mice spent significantly less time in the light zone compared to the AAV-GFP group (Fig. 4P), with no significant differences in distance travelled in light zone (Fig. 4Q). These results suggest that overexpression of Nesfatin-1 in the PVN can induce HPA axis hyperactivity and anxiety-like behaviors.

Nesfatin-1 regulates the expression of CRH

To further explore the molecular mechanism through which HT induces HPA axis dysfunction through Nesfatin-1, we investigated the regulatory effect of Nesfatin-1 on CRH, the initiating factor of the HPA axis. Here, we achieved overexpression or knockdown of Nesfatin-1 in N2a cells through transfection (Fig. 5A, G). After 48 h of transfection, we observed the fluorescence in the cells (Fig. 5B, H) and measured the mRNA and protein levels of Nesfatin-1 and CRH. In cells transfected with the plasmid overexpressing Nesfatin-1,

we found a significant increase in Nesfatin-1 and CRH mRNA and protein levels compared to the Plasmid-NC group (Fig. 5C–F). Similarly, in cells transfected with the shRNA targeting Nesfatin-1, we observed a significant decrease in Nesfatin-1 and CRH mRNA and protein levels compared to the Plasmid-NC group (Fig. 5I–L). These results suggest that Nesfatin-1 positively regulate the expression of CRH.

Surgical trauma and subsequent EA induce alterations in the hypothalamic transcriptional profile

To investigate the potential mechanisms underlying surgical trauma-induced HPA axis hyperactivity, anxiety, and the therapeutic effects of EA, we conducted RNA sequencing on hypothalamic tissues 24 h after HT in rats. The PCA analysis suggested that the Intact, HT, and EA groups were distributed separately (Fig. 6A).

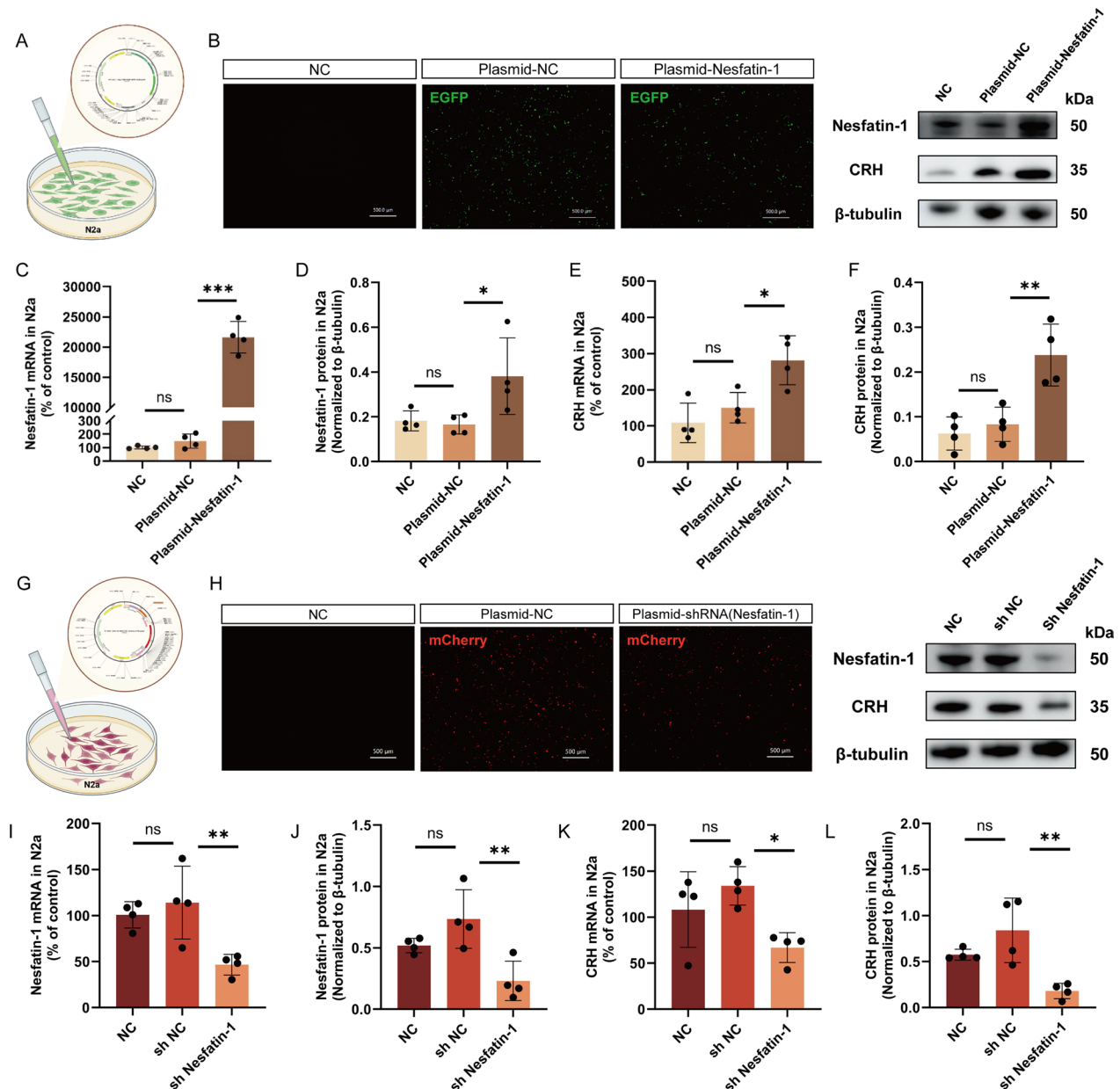


Fig. 5 Regulation of CRH expression by Nesfatin-1. **A, G** Schematic representation of plasmid transfection. **B, H** Fluorescent images of N2a cells after 48 h of plasmid transfection. Scale bar = 500 μ m. **C, D, I, J** Expression levels of Nesfatin-1 mRNA and protein in cells from each group. **E, F, K, L** Expression levels of CRH mRNA and protein in cells from each group. All data are shown as mean \pm SEM, n = 4 in each group, * $p < 0.05$, ** $p < 0.01$, *** $p < 0.001$

The transcriptional profiles differed among the three groups, and samples within the same group clustered together (Fig. 6E). The results revealed 1983 differentially expressed genes (1265 upregulated, 718 downregulated) between the HT and Intact groups (Fig. 6B). For the HT+EA group compared to the HT group, there were 742 differentially expressed genes (197 upregulated, 545 downregulated) (Fig. 6C). Among these significantly changed genes, 557 were unique to the EA (Fig. 6D).

Subsequently, KEGG pathway enrichment analysis was performed on the differentially expressed genes (fold change > 1.5, adjusted p < 0.05). The analysis revealed that the mitogen-activated protein kinase (MAPK) and cAMP signaling pathways were regulated after surgical trauma and EA (Fig. 6H, I). These pathways could activate downstream extracellular ERK and CREB pathways. The significant upregulation of genes related to the Nesfatin-1/ERK/CREB pathway and the MAPK signaling pathway is

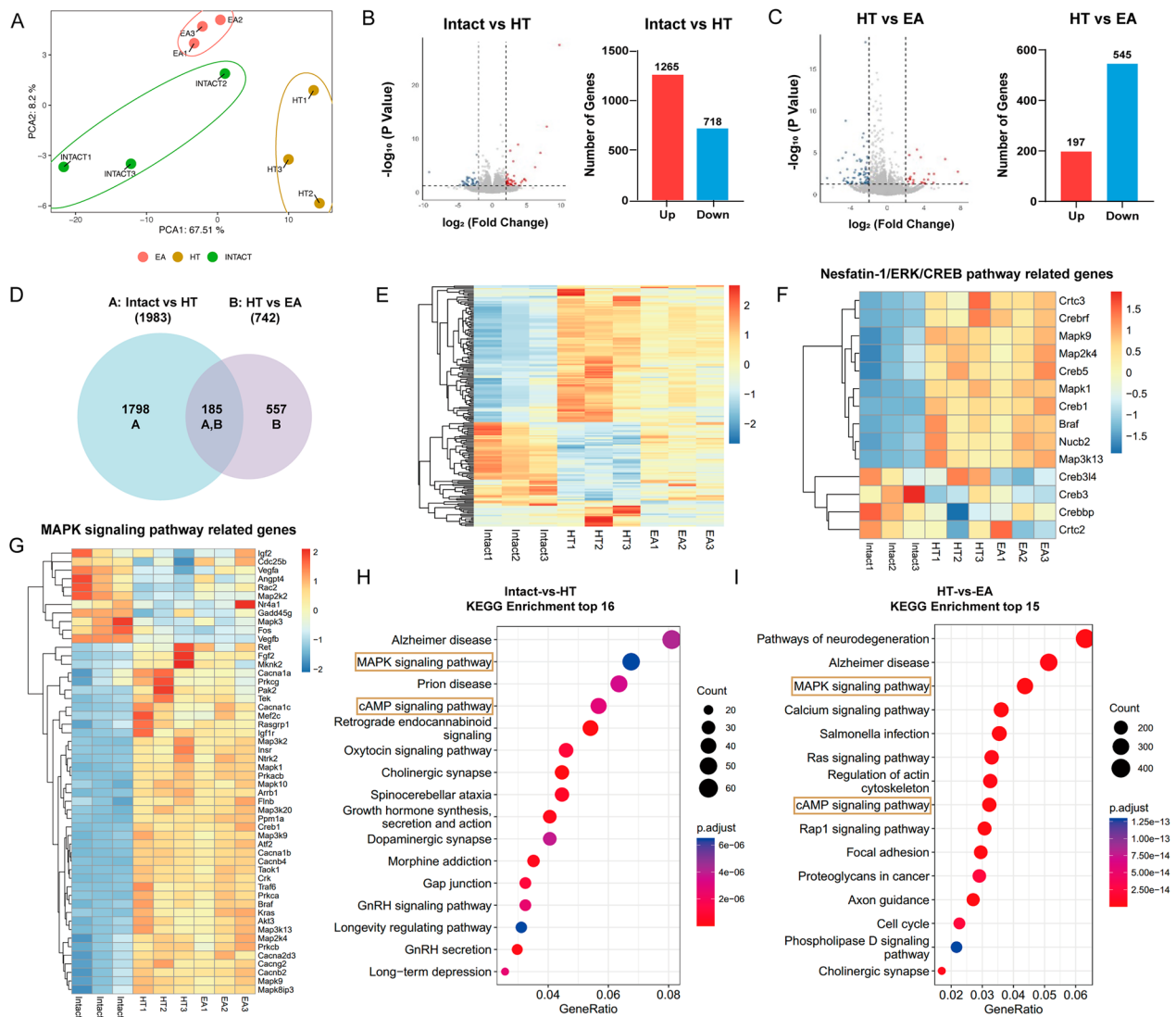


Fig. 6 Depicts the distinct transcriptional profiles induced by surgical trauma and subsequent EA treatment. **A** PCA of the PVM. **B, C** Volcano plots illustrating the upregulated and downregulated genes after surgical trauma and subsequent EA treatment, showing the number of upregulated and downregulated genes in each condition (n = 3 mice per group; fold change > 1.5, adjusted p < 0.05). **D** Venn diagram showing the unique differentially expressed genes in the HT and EA + HT groups (n = 3 mice per group; fold change > 1.5, adjusted p < 0.05). **E** Heatmap of differentially expressed genes in the hypothalamus among the Control, HT, and EA + HT groups (n = 3 mice per group; fold change > 1.5, adjusted p < 0.05). **F, G** Heatmap of differentially expressed transcripts related to the Nesfatin-1/ERK/CREB pathway and MAPK pathway (n = 3 mice per group; fold change > 1.5, adjusted p < 0.05). **H, I** KEGG pathway analysis of differentially expressed genes (fold change > 1.5, adjusted p < 0.05) after surgical trauma and subsequent EA treatment

consistent with previous studies [32, 33] (Fig. 6F, G). This suggests that the hypothalamic changes induced by surgical trauma and EA may be mediated through the ERK/CREB pathway.

Nesfatin-1 regulates CRH expression by activating the ERK/CREB pathway

Based on the transcriptome sequencing results, we first investigated whether Nesfatin-1 could modulate the ERK/CREB pathway. We injected AAV-Nesfatin-1 into the PVN to achieve overexpression of Nesfatin-1 (Fig. 3A). Upon confirming successful overexpression of Nesfatin-1 (Fig. 3B–D), we observed a significant increase in phosphorylation levels of ERK and CREB in the hypothalamus of mice in the AAV-Nesfatin-1 group compared to the AAV-GFP group (Fig. 7A–C). Concurrently, we performed plasmid transfection of N2a cells to achieve overexpression of Nesfatin-1 (Fig. 5A). Following

confirmation of successful overexpression of Nesfatin-1 (Fig. 5C, D), we observed a significant increase in phosphorylation levels of ERK and CREB in cells of the Nesfatin-1 overexpressing group compared to the control group (Fig. 7D–F). These results confirm the sufficiency of Nesfatin-1 in activating the ERK/CREB pathway.

To further investigate the role of the ERK/CREB pathway in Nesfatin-1-mediated CRH secretion, we treated N2a cells with different concentrations of ERK inhibitor (SCH772984) and CREB inhibitor (666–15) concurrently with Nesfatin-1 overexpression. We observed that compared to 0.5 μm and 1 μm concentrations, 0.25 μm of SCH772984 and 666–15 exhibited significantly stronger inhibitory effects on the elevation of CRH mRNA (Fig. 7G, H) and protein (Fig. 7I, J) induced by Nesfatin-1 overexpression. These results validate the necessity of the ERK/CREB pathway in mediating the increase in CRH induced by Nesfatin-1.

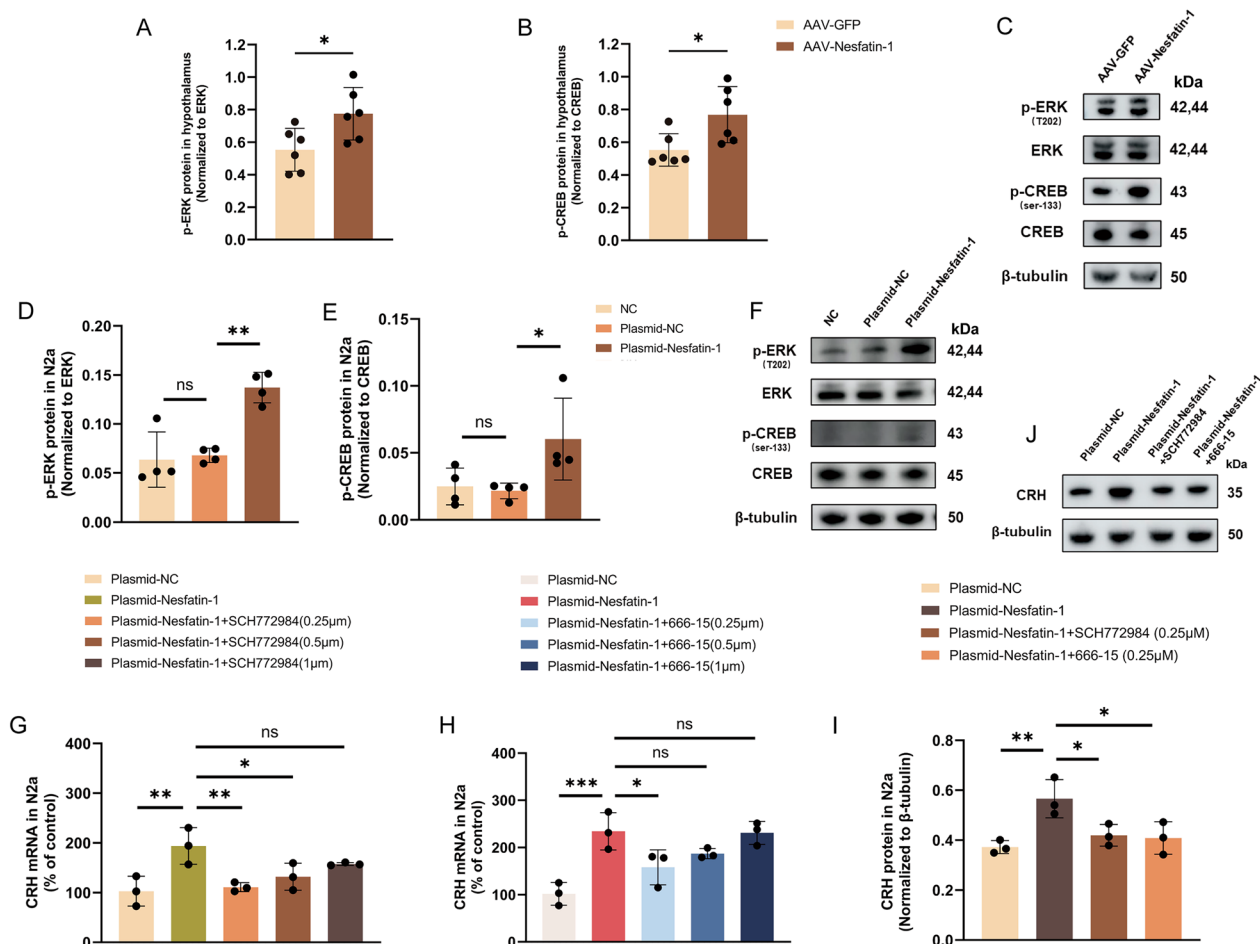


Fig. 7 Nesfatin-1 regulates CRH expression by activating the ERK/CREB pathway. **A–C** The phosphorylation levels of ERK and CREB in hypothalamus from each group. **D–F** The phosphorylation levels of ERK and CREB in N2a cells from each group. **G–H** Levels of CRH mRNA in N2a cells from each group. **I–J** Levels of CRH protein in N2a cells from each group. All data are shown as mean ± SEM, n = 3–6 in each group, * p < 0.05, ** p < 0.01, ***p < 0.001

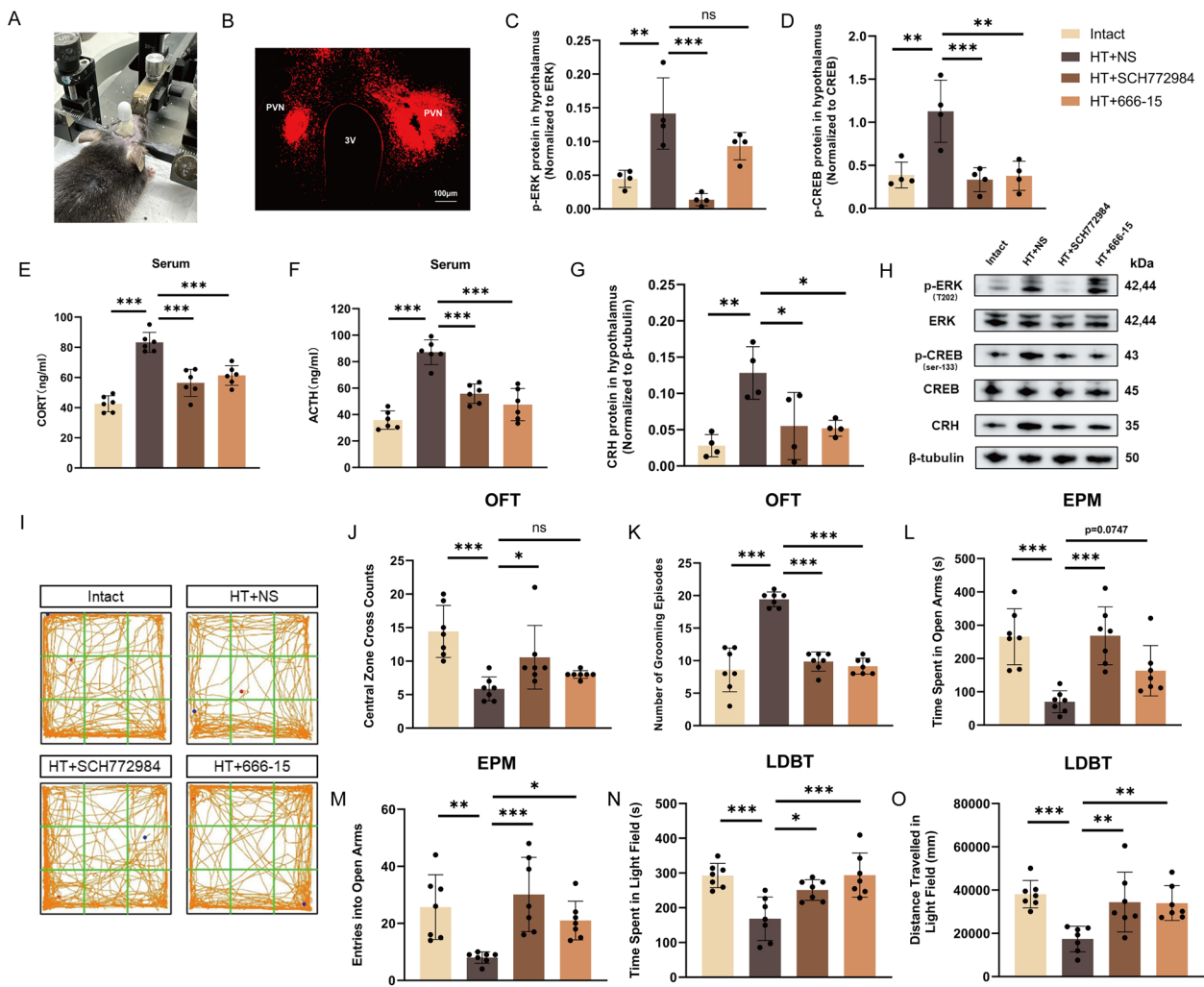


Fig. 8 Inhibition of ERK and CREB alleviates the HPA axis hyperactivity and anxiety-like behaviors caused by surgical trauma. **A** Stereotactic cannula implantation. **B** Diagram illustrating the sites of drug administration. Scale bar = 100 μ m. **C, D, G, H** The phosphorylation levels of ERK and CREB and CRH protein level in hypothalamus from each group. **E, F** Serum levels of ACTH and CORT in different groups. OFT (**I–K**), EPM (**L, M**), and LDBT (**N, O**) were used to assess anxiety levels in different groups of mice. All data are shown as mean \pm SEM, $n=4-7$ in each group, * $p<0.05$, ** $p<0.01$, *** $p<0.001$

Inhibition of ERK and CREB alleviates the HPA axis hyperactivity and anxiety-like behaviors caused by surgical trauma

We administered 0.25 μ m of SCH772984, 666–15 and NS into the PVN (Fig. 8A, B). The results showed that SCH772984 significantly decreased the phosphorylation levels of ERK and CREB in the hypothalamus of HT + NS mice (Fig. 8C, D), while 666–15 significantly reduced the phosphorylation level of CREB in the hypothalamus of these mice (Fig. 8D). Both drugs significantly reverse the increase of serum CORT, ACTH, and hypothalamic CRH protein levels induced by surgical trauma (Fig. 8E–H). These results indicate that activation of the hypothalamic ERK/CREB pathway is

necessary for the hyperactivity of the HPA axis in mice subjected to surgical trauma.

Furthermore, we assessed behavioral indices in mice after administration of the inhibitors. OFT results revealed that both inhibitors significantly reversed the decrease in central zone cross counts and the increase of grooming episodes in HT + NS mice (Fig. 8I–K). EPM results indicated that both inhibitors significantly reversed the decrease in time spent in the open arms and entries into the open arms in HT + NS mice (Fig. 8L, M). LDBT results demonstrated that both inhibitors significantly reversed the decrease in time spent and distance traveled in the light area in HT + NS mice (Fig. 8N, O). These results suggest that activation of the hypothalamic

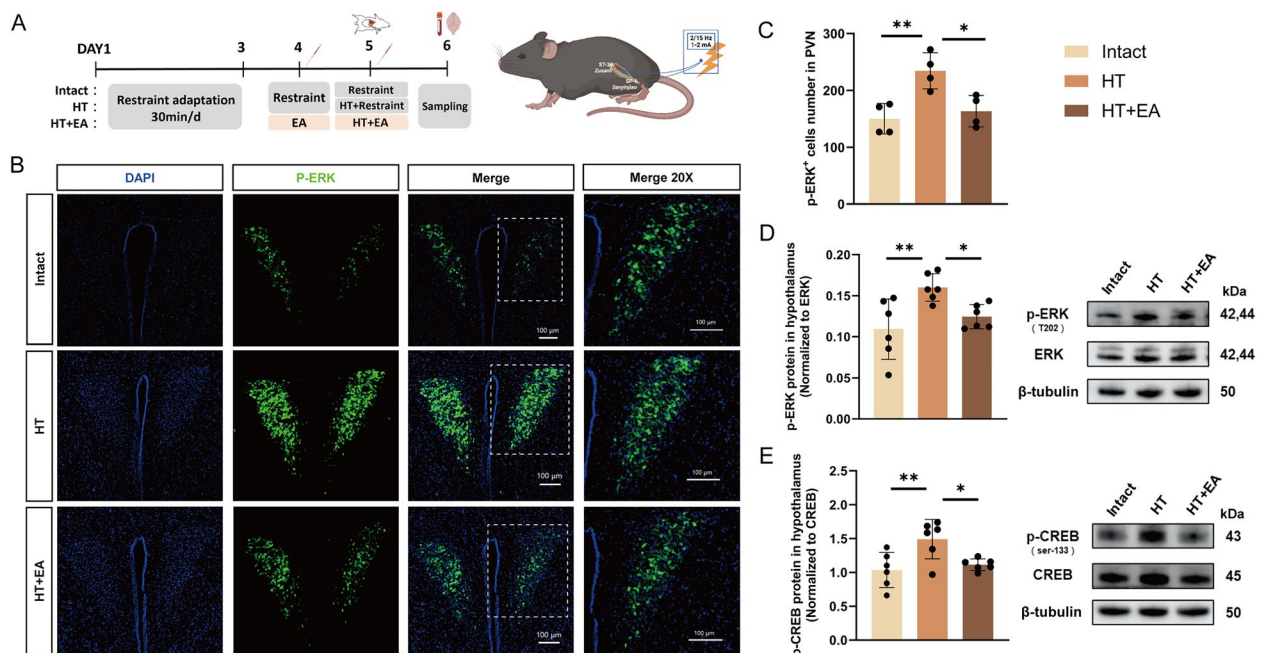


Fig. 9 EA alleviates the activation of the hypothalamic ERK/CREB pathway induced by surgical trauma. **A** Schematic representation of the HT model and EA protocol. **B** Immunofluorescent staining of p-ERK and DAPI in the PVN of mice from the Intact, HT, and EA + HT groups 24 h post-surgery. Scale bar = 100 μ m. **C** Quantification of p-ERK-positive cells in each group 24 h post-surgery. **D** Phosphorylation levels of ERK in the hypothalamus in each group. **E** Phosphorylation levels of CREB in the hypothalamus in each group. All data are shown as mean \pm SEM, $n=4-6$ in each group, * $p < 0.05$, ** $p < 0.01$, *** $p < 0.001$

ERK/CREB pathway is necessary for anxiety-like behaviors in mice subjected to surgical trauma.

EA inhibits surgical trauma-induced activation of the hypothalamic ERK/CREB pathway

We examined the changes in the hypothalamic ERK/CREB signaling pathway in mice subjected to surgical trauma and subsequent EA. The experimental workflow is depicted in Fig. 9A. Compared to the Intact mice, the HT mice exhibited a significant increase in the number of PVN p-ERK-positive cells, as well as elevated phosphorylation levels of hypothalamic ERK and CREB (Fig. 9B–E). Importantly, these increases were effectively suppressed by EA (Fig. 9B–E). This confirms that the activation of the hypothalamic ERK/CREB pathway induced by surgical trauma could be inhibited by EA.

Discussion

This study clarifies the role of EA in reducing hyperactivity of the HPA axis and consequent anxiety triggered by acute surgical trauma. Utilizing virological tools and a combination of in vitro and in vivo experiments, we have conclusively established that Nesfatin-1 plays a crucial role in mediating the effects of EA on both endocrine and emotional disturbances. Moreover, we have identified ERK and CREB as key molecules in the

Nesfatin-1-mediated regulation of CRH. The Nesfatin-1/ERK/CREB pathway is effectively downregulated by the EA treatment, leading to the alleviation of trauma-induced HPA axis hyperactivity and subsequent anxiety.

The HPA axis plays a crucial role in regulating homeostasis and responses to threats from both internal and external environments. However, excessive activation of the HPA axis often leads to a series of harmful effects and adverse reactions [34]. Surgical trauma, as a form of acute stress, can lead to HPA axis hyperactivity. Partial HT induces tissue ischemia, hypoxia, as well as abnormalities in endocrine, metabolic, and immune functions, providing a robust simulation of surgical stress response [35]. In this study we employed a partial HT model to simulate surgical trauma. The impact of HT model on the HPA axis function has been preliminarily explored. Our previous studies indicated varying degrees of HPA axis hyperactivity at 2 h, 4 h, 6 h, 24 h, and 72 h after HT in rats [35, 36]. Hyperactivity of HPA axis can result in endocrine disruption and serve as the primary initiating factor for severe secondary injuries such as systemic inflammatory response syndrome and multiple organ dysfunction syndrome [37]. CRH, secreted by parvocellular neurons in the PVN, acts as the “gate-keeper” for initiating HPA axis and is a significant factor contributing to anxiety [38, 39]. Studies have shown

elevated central CRH levels in stress-related anxiety and depressive patients, with normalization observed after treatment [40]. Corticotropin releasing hormone receptor 1 (CRHR1) antagonists such as antalarmin [41] and miR-34b, which targets CRHR1 and negatively regulates its mRNA [30], have been reported to alleviate anxiety. Additionally, anxiety patients exhibit evident HPA axis hyperactivity, and chronic activation of the HPA axis has been linked to the development and exacerbation of anxiety [42]. Therefore, the excessive secretion of PVN CRH, causing HPA axis hyperactivity, deserves attention due to its role in inducing anxiety and adverse consequences following surgical trauma. Here, we observed HPA axis activation after surgery, evidenced by elevated PVN CRH levels and increased serum ACTH and CORT levels. Similarly, through behavioral experiments, mice exhibited pronounced anxiety-like behaviors, consistent with previous experimental results [30].

A significant body of research indicates that EA has a favorable anti-stress effect by regulating the HPA axis. In various conditions such as anxiety and depression [43], cardiovascular diseases [10], immune suppression [44], irritable bowel syndrome [45] and diabetes [46], the use of EA has been shown to alleviate HPA axis hyperactivity, achieving therapeutic benefits. During the perioperative period, the application of EA can alleviate preoperative anxiety and tension in patients, reduce the use of anesthetics during surgery [47], and effectively relieve postoperative pain and gastrointestinal discomfort [12, 48]. Studies have shown that preoperative acupuncture is an effective intervention to alleviate patient anxiety [13]. Additionally, EA before gynecological laparoscopic surgery can improve postoperative analgesia and reduce postoperative side effects [49]. The selection of acupoints is a crucial factor influencing the efficacy of EA. ST36 and SP6 are the most commonly used acupoint combinations in clinical practice [50]. Studies indicate that EA at ST36 can alleviate anxiety and depression levels in rats subjected to unpredictable chronic mild stress (UCMS) by regulating the HPA axis [51]. Meanwhile, our previous research indicated that non-acupoint intervention (where acupuncture needles are inserted into the ipsilateral tail root and electrical stimulation is applied) failed to improve HPA axis dysfunction in traumatized animals [52]. Our research confirms that preoperative EA pretreatment combined with postoperative EA can effectively alleviate HPA axis hyperactivity and anxiety.

Although the beneficial regulatory effects of EA on the HPA axis have been widely confirmed, its specific mechanisms remain unclear. Previous studies have indicated that EA can enhance the inhibitory regulation of the hypothalamic gamma-aminobutyric acid-A receptor $\alpha 3$ subunit [18], inhibit the phosphorylation of hypothalamic

N-methyl-D-aspartate receptor 2A [29], thereby reducing excessive secretion of CRH, and alleviate HPA axis hyperactivity induced by surgical trauma. Recent research also suggests that EA can reverse the downregulation of hypothalamic oxytocin and oxytocin receptor induced by surgical trauma, downregulate glucocorticoid receptor expression [17], and impact the circRNA-miRNA-mRNA network [19], suppressing HPA axis hyperactivity. In this study, we investigated the role of a novel neuropeptide, Nesfatin-1, in surgical trauma. Nesfatin-1, first discovered in the hypothalamus in 2006, is derived from NUCB2 [53] and consists of three domains: N-terminal, middle portion (M30), and C-terminal, with M30 playing a crucial role in inducing physiological effects [54]. Previous studies have indicated that Nesfatin-1 plays a significant role in stress regulation. Co-localization of Nesfatin-1 and CRH in the PVN has been observed [55]. Nesfatin-1 neurons in multiple stress-related brain regions, including the PVN, are significantly activated in various stress conditions such as restraint stress [56], water avoidance stress [57], abdominal surgery [58], and lipopolysaccharide injection [59]. Three weeks of UCMS in rats leads to a significant increase in Nesfatin-1 and CRH mRNA levels in the hypothalamus, as well as elevated serum CORT levels [60]. Central injection of Nesfatin-1 induces enhanced HPA axis and sympathetic nervous system activity [61], anxiety-like behaviors [26, 62], and changes in visceral function [63]. In human studies, high levels of Nesfatin-1 have been detected in the plasma of individuals diagnosed with severe depression [64], and serum Nesfatin-1 in obese women correlates positively with perceived stress, anxiety, and depression levels [65]. These findings suggest the involvement of Nesfatin-1 in the regulation of stress and stress-related psychiatric disorders. Our research results showed that in HT mice, Nesfatin-1 expression in the hypothalamus significantly increased, and EA reduced its elevated expression. Furthermore, stereotactic injection of Nesfatin-1 overexpression virus into the PVN could simulate HPA axis hyperactivity and anxiety-like behaviors induced by surgical trauma, while Nesfatin-1 knockdown virus could inhibit HPA axis hyperactivity and anxiety-like behaviors induced by surgical trauma, like the effects of EA. This indicates that EA has the potential to alleviate HPA axis hyperactivity and anxiety after surgical trauma by inhibiting the elevated levels of endogenous Nesfatin-1 in the hypothalamus.

Although the receptors for Nesfatin-1 have not been definitively identified, the intracellular signaling pathways induced by Nesfatin-1 have been extensively studied [66]. In our experiment, we clarified the positive regulatory effect of Nesfatin-1 on CRH in N2a cells and used transcriptome sequencing to explore the downstream

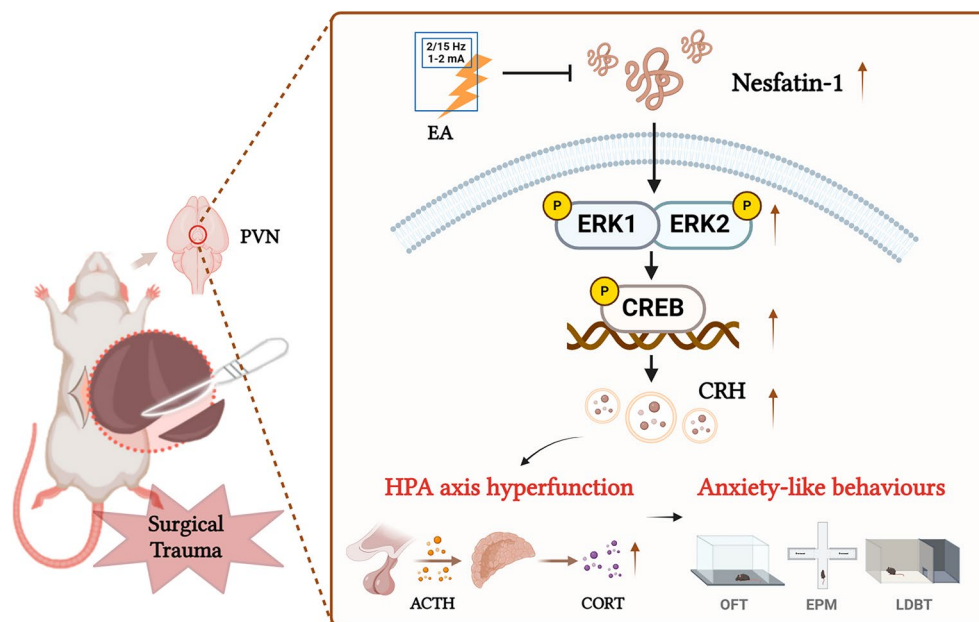


Fig. 10 Electroacupuncture modulates Nesfatin-1/ERK/CREB pathway to reduce surgical trauma-induced HPA axis hyperactivity and anxiety. Figure created with BioRender.com

signaling pathways mediated by Nesfatin-1. ERK is a member of the MAPK family and plays a crucial role in transmitting surface receptor signals to the cell nucleus [67]. CREB is a cAMP response element-binding protein that selectively binds to cAMP response elements (CRE), regulating the transcription of various cellular genes. Transcriptome sequencing revealed that genes significantly altered by HT and EA were enriched in the MAPK and cAMP signaling pathways, both of which activated downstream ERK and CREB. In the PVN, ERK could phosphorylate CREB and promote its translocation to the nucleus, where it binds with CRE to activate the transcription of CRH [68]. Studies have shown that Nesfatin-1 treatment of SH-SY5Y cells increases the phosphorylation of ERK1/2 and CRH levels [69]. Microinjection of Nesfatin-1 into the PVN of rats increases the number of p-ERK1/2-positive cells and CRH levels [70]. Treatment of NB41A3 cells with Nesfatin-1 or M30 increases the phosphorylation levels of CREB [71]. Our research results show that overexpression of Nesfatin-1 in N2a cells could activate the ERK/CREB pathway, and application of ERK or CREB inhibitors could reverse the increase in CRH caused by Nesfatin-1 overexpression. EA, on other hand inhibits the activation of the hypothalamic ERK/CREB pathway induced by surgical trauma. Microinjection of ERK or CREB inhibitors into the PVN of mice can alleviate HPA axis hyperactivity and anxiety-like behaviors caused by surgical trauma, similar to the effects of EA. This suggests that the Nesfatin-1/ERK/CREB pathway is involved in HPA axis hyperactivity and

anxiety caused by surgical trauma and can be inhibited by EA.

The HPA axis undergoes dynamic changes and exhibits a circadian rhythm. In this study, we only explored the time point of 24 h after surgery, which may not provide a comprehensive understanding. Additionally, although mice showed good recovery 24 h postoperatively, the abdominal incision is likely to affect their motor function. Therefore, we corrected the OFT data, focusing on the ratio of the distance moved in the central area to the total distance moved and the speed during movement, rather than average speed. It is worth noting that these indicators were significantly improved after EA treatment, which may extend beyond the regulatory effect of EA on the HPA axis, involving overall regulation, including anti-inflammatory and analgesic effects, aligning with traditional Chinese medicine principles. Furthermore, gender differences were not considered in this study. Since research has indicated that expression of Nesfatin-1 seems to be higher in the brains of males than females with depression [55]. However, our experiment only investigated male mice. These limitations should be thoroughly addressed in future research endeavors.

Conclusion

In conclusion, our study demonstrates that the hypothalamic Nesfatin-1/ERK/CREB pathway may be involved in the inhibitory effects of EA on surgical trauma-induced HPA axis hyperactivity and anxiety (Fig. 10).

Abbreviations

ACTH	Adrenocorticotrophic hormone
CRE	CAMP response elements
CRH	Corticotropin-releasing hormone
CRHR1	Corticotropin releasing hormone receptor 1
CORT	Corticosterone
CREB	CAMP-response element binding protein
EA	Electroacupuncture
EPM	Elevated plus maze
ERK	Extracellular regulated protein kinases
HPA	Hypothalamic–pituitary–adrenal
HT	Hepatectomy
LDBT	Light–dark box tests
MAPK	Mitogen-activated protein kinase
M30	Middle portion
NS	Normal saline
NUCB2	Nucleobindin2
N2a	Neuroblastoma-2a
OFT	Open field tests
PAC	Principal component analysis
PVN	Paraventricular nucleus
SD	Sprague–Dawley
UCMS	Unpredictable chronic mild stress
3V	Third ventricle

Supplementary Information

The online version contains supplementary material available at <https://doi.org/10.1186/s13020-024-00974-2>.

Supplementary Material 1.

Acknowledgements

We acknowledge Assoc. Prof. Jun Wang for her suggestions on the experiments as well as Jing Han, Tongtong Zhang, Yi Jiang, Wei Hu, Xiaoqiang Zhao and Hao Sun for their technical help. We also appreciate the technical support provided by the Shanghai Key Laboratory for Acupuncture Mechanism and Acupoint Function (No.21DZ2271800).

Author contributions

ZZT designed the project and supervised the research. JYZ and AJZ performed the molecular biology experiments. JYZ, YXZ and YHX conducted the behavioral tests. JYZ and CZ undertook the statistical analysis. CZ performed bioinformatics analyses and helped with manuscript language polishing. JYZ and YW wrote the manuscript. ZZT and JY reviewed and revised the manuscript. All authors read and approved the final manuscript.

Funding

This work was supported by the National Natural Science Foundation of China (Grants numbers 82474210, 81973639 and 81573712) and the Innovative Research Team of High-level Local Universities in Shanghai.

Availability of data and materials

The datasets used or analyzed throughout this study are available from the corresponding author upon reasonable request.

Declarations

Ethics approval and consent to participate

All animal experiments were reviewed and approved by the Ethics Committee for Laboratory Animals, School of Basic Medical Sciences, Fudan University (20240229–050).

Consent for publication

All authors agreed with the content of the manuscript and approved the final version of the manuscript.

Competing interests

The authors report no competing interests in this work.

Author details

¹Department of Integrative Medicine and Neurobiology, School of Basic Medical Sciences, State Key Laboratory of Medical Neurobiology and MOE Frontiers Center for Brain Science, Institutes of Brain Science, Institute of Acupuncture Research, Academy of Integrative Medicine, Shanghai Key Laboratory for Acupuncture Mechanism and Acupoint Function, Shanghai Medical College, Fudan University, Shanghai 200032, China. ²Department of Medical Oncology, Zhongshan Hospital, Fudan University, Shanghai 200032, China. ³Department of Rehabilitation Medicine, Huashan Hospital, Fudan University, Shanghai 200040, China. ⁴Department of Neurological Rehabilitation Medicine, The First Rehabilitation Hospital of Shanghai, Shanghai 200090, China.

Received: 29 April 2024 Accepted: 29 July 2024

Published: 17 August 2024

References

- Cerejeira J, Batista P, Nogueira V, Vaz-Serra A, Mukaetova-Ladinska EB. The stress response to surgery and postoperative delirium: evidence of hypothalamic-pituitary-adrenal axis hyperresponsiveness and decreased suppression of the GH/IGF-1 axis. *J Geriatr Psychiatry Neurol*. 2013;26(3):185–94.
- Gibbison B, Angelini GD, Lightman SL. Dynamic output and control of the hypothalamic-pituitary-adrenal axis in critical illness and major surgery. *Br J Anaesth*. 2013;111(3):347–60.
- Rasiah NP, Loewen SP, Bains JS. Windows into stress: a glimpse at emerging roles for CRH(PVN) neurons. *Physiol Rev*. 2023;103(2):1667–91.
- Desborough JP. The stress response to trauma and surgery. *Br J Anaesth*. 2000;85(1):109–17.
- Orci LA, Toso C, Mentha G, Morel P, Majno PE. Systematic review and meta-analysis of the effect of perioperative steroids on ischaemia-reperfusion injury and surgical stress response in patients undergoing liver resection. *Br J Surg*. 2013;100(5):600–9.
- Zhao Q, Shen Y, Li R, Wu J, Lyu J, Jiang M, et al. Cardiac arrest and resuscitation activates the hypothalamic-pituitary-adrenal axis and results in severe immunosuppression. *J Cereb Blood Flow Metab*. 2021;41(5):1091–102.
- Suzuki M, Deno M, Myers M, Asakage T, Takahashi K, Saito K, et al. Anxiety and depression in patients after surgery for head and neck cancer in Japan. *Pall Supp Care*. 2016;14(3):269–77.
- Oteri V, Martinelli A, Crivellaro E, Gigli F. The impact of preoperative anxiety on patients undergoing brain surgery: a systematic review. *Neurosurg Rev*. 2021;44(6):3047–57.
- Xiao Y, Chen Y, Feng Y, Lee K. Advances in neural mechanisms related to acupuncture sensation. *Tradit Med Modern Med*. 2022;05(01n04):1–12.
- Ye Z, Zhu L, Li XJ, Gao HY, Wang J, Wu SB, et al. PC6 electroacupuncture reduces stress-induced autonomic and neuroendocrine responses in rats. *Heliyon*. 2023;9(4):e15291.
- Wang K, Yong Y, Zhou J, Zhou WX, Guo J, Chen TY. Electroacupuncture attenuates surgical stress-induced reduction of T lymphocytes through modulation of peripheral opioid system. *Chin J Integr Med*. 2021;27(2):98–105.
- Zhang W, Zhang H, Wang S-M, Guo J, Ma Y, Li Y, et al. Perioperative acupuncture optimizes surgical outcomes: theory, clinical practice and future perspectives. *Am J Chin Med*. 2022;50(04):961–78.
- Tong Q-Y, Liu R, Zhang K, Gao Y, Cui G-W, Shen W-D. Can acupuncture therapy reduce preoperative anxiety? A systematic review and meta-analysis. *J Integr Med*. 2021;19(1):20–8.
- Wu M, Chen Y, Shen Z, Zhu Y, Xiao S, Zhu X, et al. Electroacupuncture alleviates anxiety-like behaviors induced by chronic neuropathic pain via regulating different dopamine receptors of the basolateral amygdala. *Mol Neurobiol*. 2022;59(9):5299–311.
- Zheng J, Zhu J, Wang Y, Tian Z. Effects of acupuncture on hypothalamic-pituitary-adrenal axis: current status and future perspectives. *J Integr Med*. 2024;22(4):445–458. <https://doi.org/10.1016/j.joim.2024.06.004>.
- Zhang M, Sun J, Wang Y, Tian Z. Secretagogin mediates the regulatory effect of electroacupuncture on hypothalamic-pituitary-adrenal axis dysfunction in surgical trauma. *Neural Plast*. 2021;2021:8881136.
- Wu F, Zhu J, Wan Y, Subinuer K, Zhou J, Wang K, et al. Electroacupuncture ameliorates hypothalamic-pituitary-adrenal axis dysfunction induced

- by surgical trauma in mice through the hypothalamic oxytocin system. *Neurochem Res.* 2023;48(11):3391–3401. <https://doi.org/10.1007/s11064-023-03984-y>.
18. Zhu L, Zhu J, Chen Z, Meng Z, Ju M, Zhang M, et al. Electroacupuncture (EA) speeds up the regulation of hypothalamic pituitary adrenal axis dysfunction in acute surgical trauma rats: mediated by hypothalamic gamma-aminobutyric acid GABA-A receptors. *J Behav Brain Sci.* 2018;08(12):697–710.
 19. Wang Y, Hu W, Han J, Zheng J, Jiang N, Feng Y, et al. Electroacupuncture alleviates perioperative hypothalamus-pituitary-adrenal axis dysfunction via circRNA-miRNA-mRNA networks. *Front Mol Neurosci.* 2023;16:1115569.
 20. Weibert E, Hofmann T, Stengel A. Role of nesfatin-1 in anxiety, depression and the response to stress. *Psychoneuroendocrinology.* 2019;100:58–66.
 21. Zheng J, Han J, Wang Y, Tian Z. Role of brain NUCB2/nesfatin-1 in stress and stress-related gastrointestinal disorders. *Peptides.* 2023;167:171043.
 22. Emmerzaal TL, Kozicz T. Nesfatin-1; implication in stress and stress-associated anxiety and depression. *Curr Pharm Des.* 2013;19(39):6941–8.
 23. Ozcan M, Gok ZB, Kacar E, Serhatlioglu I, Kelestimur H. Nesfatin-1 increases intracellular calcium concentration by protein kinase C activation in cultured rat dorsal root ganglion neurons. *Neurosci Lett.* 2016;619:177–81.
 24. Kőnczöl K, Bodnár I, Zelena D, Pintér O, Papp RS, Palkovits M, et al. Nesfatin-1/NUCB2 may participate in the activation of the hypothalamic-pituitary-adrenal axis in rats. *Neurochem Int.* 2010;57(3):189–97.
 25. Yoshida N, Maejima Y, Sedbazar U, Ando A, Kurita H, Damdindorj B, et al. Stressor-responsive central nesfatin-1 activates corticotropin-releasing hormone, noradrenaline and serotonin neurons and evokes hypothalamic-pituitary-adrenal axis. *Aging.* 2010;2(11):775–84.
 26. Merali Z, Cayer C, Kent P, Anisman H. Nesfatin-1 increases anxiety- and fear-related behaviors in the rat. *Psychopharmacology.* 2008;201(1):115–23.
 27. Schalla MA, Kühne SG, Friedrich T, Kobelt P, Goebel-Stengel M, Long M, et al. Central blockage of nesfatin-1 has anxiolytic effects but does not prevent corticotropin-releasing factor-induced anxiety in male rats. *Biochem Biophys Res Commun.* 2020;529(3):773–7.
 28. Zhu J, Wang C, Wang Y, Guo C, Lu P, Mou F, et al. Electroacupuncture alleviates anxiety and modulates amygdala CRH/CRHR1 signaling in single prolonged stress mice. *Acupunct Med.* 2022;40(4):369–78.
 29. Wang Y, Han J, Zhu J, Zhang M, Ju M, Du Y, et al. GluN2A/ERK/CREB signaling pathway involved in electroacupuncture regulating hypothalamic-pituitary-adrenal axis hyperactivity. *Front Neurosci.* 2021;15:703044.
 30. Zhu J, Chen Z, Tian J, Meng Z, Ju M, Wu G, et al. miR-34b attenuates trauma-induced anxiety-like behavior by targeting CRHR1. *Int J Mol Med.* 2017;40(1):90–100.
 31. Ji N-N, Cao S, Song X-L, Pei B, Jin C-Y, Fan B-F, et al. Glutamatergic neurons in the paraventricular nucleus of the hypothalamus participate in the regulation of visceral pain induced by pancreatic cancer in mice. *Hepatobiliary Surg Nutr.* 2023;13(2):258–272. <https://doi.org/10.2103/hbsn-23-442>.
 32. Rao J, Li H, Zhang H, Xiang X, Ding X, Li L, et al. *Periplaneta Americana* (L.) extract activates the ERK/CREB/BDNF pathway to promote post-stroke neuroregeneration and recovery of neurological functions in rats. *J Ethnopharmacol.* 2024;321:117400. <https://doi.org/10.1016/j.jep.2023.117400>.
 33. Huang H, Li Y, Wang X, Zhang Q, Zhao J, Wang Q. Electroacupuncture pretreatment protects against anesthesia/surgery-induced cognitive decline by activating CREB via the ERK/MAPK pathway in the hippocampal CA1 region in aged rats. *Aging.* 2023;15(20):11227–43.
 34. Walker BR. Glucocorticoids and cardiovascular disease. *Eur J Endocrinol.* 2007;157(5):545–59.
 35. Zhu J, Chen Z, Zhu L, Meng Z, Wu G, Tian Z. arginine vasopressin and arginine vasopressin receptor 1b involved in electroacupuncture-attenuated hypothalamic-pituitary-adrenal axis hyperactivity in hepatectomy rats. *Neuromodulation.* 2016;19(5):498–506.
 36. Zhu J, Chen Z, Meng Z, Ju M, Zhang M, Wu G, et al. Electroacupuncture alleviates surgical trauma-induced hypothalamus pituitary adrenal axis hyperactivity via microRNA-142. *Front Mol Neurosci.* 2017;10:308.
 37. Zhuang CL, Chen FF, Lu JX, Zhang BS, Liu S, Zhou CJ, et al. Impact of different surgical traumas on postoperative ileus in rats and the mechanisms involved. *Int J Clin Exp Med.* 2015;8(9):16778–86.
 38. Herman JP, McKlveen JM, Ghosal S, Kopp B, Wulsin A, Makinson R, et al. Regulation of the hypothalamic-pituitary-adrenocortical stress response. *Compr Physiol.* 2016;6(2):603–21.
 39. Wu C, Zetter MA. Role of the hypothalamic paraventricular nucleus in anxiety disorders. *Stress and Brain.* 2022;2(3):53–65.
 40. Retson TA, Reyes BA, Van Bockstaele EJ. Chronic alcohol exposure differentially affects activation of female locus coeruleus neurons and the subcellular distribution of corticotropin releasing factor receptors. *Prog Neuropsychopharmacol Biol Psychiatry.* 2015;56:66–74.
 41. Tsigos C, Chrousos GP. Hypothalamic-pituitary-adrenal axis, neuroendocrine factors and stress. *J Psychosom Res.* 2002;53(4):865–71.
 42. Borrow AP, Stranahan AM, Suchecki D, Yunes R. Neuroendocrine regulation of anxiety: beyond the hypothalamic-pituitary-adrenal axis. *J Neuroendocrinol.* 2016;28(7). <https://doi.org/10.1111/jne.12403>.
 43. Liu RP, Fang JL, Rong PJ, Zhao Y, Meng H, Ben H, et al. Effects of electroacupuncture at auricular concha region on the depressive status of unpredictable chronic mild stress rat models. *Evid Based Complement Alternat Med.* 2013;2013:789674.
 44. Zhang Y, Wu GC, He QZ, Cao XD. Effect of morphine and electroacupuncture (EA) on apoptosis of thymocytes. *Acupunct Electrother Res.* 2000;25(1):17–26.
 45. Ma X-P, Tan L-Y, Yang Y, Wu H-G, Jiang B, Liu H-R, et al. Effect of electroacupuncture on substance P, its receptor and corticotropin-releasing hormone in rats with irritable bowel syndrome. *World J Gastroenterol.* 2009;15(41):5211–7. <https://doi.org/10.3748/wjg.15.5211>.
 46. Gao S, Li R, Tian HH, Pei ES, Cao BY, Wu Y. Effects of electroacupuncture at “Yishu” (EX-B 3) on the relative hormones of HPA axis in rats with type-2 diabetes mellitus. *Zhongguo Zhen Jiu.* 2014;34(11):1099–105.
 47. Qiao L, Guo M, Qian J, Xu B, Gu C, Yang Y. Research advances on acupuncture analgesia. *Am J Chin Med.* 2020;48(2):245–58.
 48. Ding Y-Y, Xu F, Wang Y-F, Han L-L, Huang S-Q, Zhao S, et al. Electroacupuncture alleviates postoperative pain through inhibiting neuroinflammation via stimulator of interferon genes/type-1 interferon pathway. *J Integr Med.* 2023;21(5):496–508.
 49. Yao Y, Zhao Q, Gong C, Wu Y, Chen Y, Qiu L, et al. Transcutaneous electrical acupoint stimulation improves the postoperative quality of recovery and analgesia after gynecological laparoscopic surgery: a randomized controlled trial. *Evid Based Complement Alternat Med.* 2015;2015:324360.
 50. Zhou F, Jiang H, Kong N, Lin J, Zhang F, Mai T, et al. Electroacupuncture attenuated anxiety and depression-like behavior via inhibition of hippocampal inflammatory response and metabolic disorders in TNBS-induced IBD rats. *Oxid Med Cell Longev.* 2022;2022:8295580.
 51. Le JJ, Yi T, Qi L, Li J, Shao L, Dong JC. Electroacupuncture regulate hypothalamic-pituitary-adrenal axis and enhance hippocampal serotonin system in a rat model of depression. *Neurosci Lett.* 2016;615:66–71.
 52. Zhu J, Guo C, Lu P, Shao S, Tu B. Contribution of growth arrest-specific 5/miR-674 to the hypothalamus pituitary adrenal axis regulation effect by electroacupuncture following trauma. *NeuroImmunoModulation.* 2021;28(3):137–49.
 53. Oh IS, Shimizu H, Satoh T, Okada S, Adachi S, Inoue K, et al. Identification of nesfatin-1 as a satiety molecule in the hypothalamus. *Nature.* 2006;443(7112):709–12.
 54. Palasz A, Krzystanek M, Worthington J, Czajkowska B, Kostro K, Wiaderkiewicz R, et al. Nesfatin-1, a unique regulatory neuropeptide of the brain. *Neuropeptides.* 2012;46(3):105–12.
 55. Bloem B, Xu L, Morava E, Faludi G, Palkovits M, Roubos EW, et al. Sex-specific differences in the dynamics of cocaine- and amphetamine-regulated transcript and nesfatin-1 expressions in the midbrain of depressed suicide victims vs. controls. *Neuropharmacology.* 2012;62(1):297–303.
 56. Okere B, Xu L, Roubos EW, Sonetti D, Kozicz T. Restraint stress alters the secretory activity of neurons co-expressing urocortin-1, cocaine- and amphetamine-regulated transcript peptide and nesfatin-1 in the mouse Edinger-Westphal nucleus. *Brain Res.* 2010;1317:92–9.
 57. Goebel-Stengel M, Wang L, Stengel A, Taché Y. Localization of nesfatin-1 neurons in the mouse brain and functional implication. *Brain Res.* 2011;1396:20–34.
 58. Stengel A, Goebel M, Wang L, Taché Y. Abdominal surgery activates nesfatin-1 immunoreactive brain nuclei in rats. *Peptides.* 2010;31(2):263–70.
 59. Bonnet MS, Pecchi E, Trouslard J, Jean A, Dallaporta M, Troadec JD. Central nesfatin-1-expressing neurons are sensitive to peripheral inflammatory stimulus. *J Neuroinflammation.* 2009;6:27.

60. Kumar A, Dogra S, Sona C, Umrao D, Rashid M, Singh SK, et al. Chronic histamine 3 receptor antagonism alleviates depression like conditions in mice via modulation of brain-derived neurotrophic factor and hypothalamus-pituitary adrenal axis. *Psychoneuroendocrinology*. 2019;101:128–37.
61. Tanida M, Mori M. Nesfatin-1 stimulates renal sympathetic nerve activity in rats. *NeuroReport*. 2011;22(6):309–12.
62. Hofmann T, Stengel A, Ahnis A, Buße P, Elbelt U, Klapp BF. NUCB2/nesfatin-1 is associated with elevated scores of anxiety in female obese patients. *Psychoneuroendocrinology*. 2013;38(11):2502–10.
63. Gu Q, Lei Y, Wu J, He T, Li J, Song S. NUCB2/Nesfatin-1 regulation of chronic visceral hyperalgesia. *Appl Bionics Biomechan*. 2022;2022:4079533.
64. Ari M, Ozturk OH, Bez Y, Oktar S, Erduran D. High plasma nesfatin-1 level in patients with major depressive disorder. *Prog Neuropsychopharmacol Biol Psychiatry*. 2011;35(2):497–500.
65. Hofmann T, Elbelt U, Ahnis A, Rose M, Klapp BF, Stengel A. Sex-specific regulation of NUCB2/nesfatin-1: differential implication in anxiety in obese men and women. *Psychoneuroendocrinology*. 2015;60:130–7.
66. Rupp SK, Wolk E, Stengel A. Nesfatin-1 receptor: distribution, signaling and increasing evidence for a G protein-coupled receptor—a systematic review. *Front Endocrinol*. 2021;12:740174.
67. Zhen W, Zhen H, Wang Y, Chen L, Niu X, Zhang B, et al. Mechanism of ERK/CREB pathway in pain and analgesia. *Front Mol Neurosci*. 2023;16:1156674. <https://doi.org/10.3389/fnmol.2023.1156674>.
68. Wang JQ, Mao L. The ERK pathway: molecular mechanisms and treatment of depression. *Mol Neurobiol*. 2019;56(9):6197–205.
69. Chen Z, Xu YY, Ge JF, Chen FH. CRHR1 mediates the up-regulation of synapsin I induced by nesfatin-1 through ERK 1/2 signaling in SH-SY5Y cells. *Cell Mol Neurobiol*. 2018;38(3):627–33.
70. Tanida M, Gotoh H, Yamamoto N, Wang M, Kuda Y, Kurata Y, et al. Hypothalamic nesfatin-1 stimulates sympathetic nerve activity via hypothalamic ERK signaling. *Diabetes*. 2015;64(11):3725–36.
71. Knoll BJ, Ishida E, Hashimoto K, Shimizu H, Okada S, Satoh T, et al. Nesfatin-1 induces the phosphorylation levels of cAMP response element-binding protein for intracellular signaling in a neural cell line. *PLoS ONE*. 2012;7(12):e50918. <https://doi.org/10.1371/journal.pone.0050918>.

Publisher's Note

Springer Nature remains neutral with regard to jurisdictional claims in published maps and institutional affiliations.